Electronic stopping power of protons and alpha particles in nickel

Edwin E. Quashie and Alfredo A. Correa

Phys. Rev. B **98**, 235122 — Published 10 December 2018

DOI: 10.1103/PhysRevB.98.235122

Electronic stopping power of protons and alpha particles in Nickel

Edwin E. Quashie and Alfredo A. Correa
Quantum Simulations Group, Lawrence Livermore National Laboratory, Livermore, California 94550, USA

The electronic stopping power of nickel for proton and alpha particles at velocities below and around the Fermi velocity has been obtained to high accuracy using time-dependent density functional theory. For the wide range of projectile velocities considered, we observed different regimes of electronic stopping due to the alternative participation of s and d-band electrons. Despite the sharp discontinuity in the electronic density of states near the Fermi energy characteristic of the nickel band structure, we do not find an anomalous non-linear electronic stopping power limit as a function of velocity. However, we find a crossover region above $v = 0.15$ a.u. both for protons and alpha, related to the increase in participating host electrons and, in the case of alpha, to an increase of the charge state. We compare our calculated results with widely available experimental data and analyze the low velocity limits in the context of Lindhard's linear response theory and previous non-linear density functional calculations. The comparison is in good accord with the lowest velocity experiments available. This may indicate that the adiabatic local density approximation is already a good theory to calculate electronic stopping power in materials at low velocity.

Various theories have been developed to calculate electronic stopping power (S_e), ranging from the early perturbative methods of Bethe, Fermi-Teller and Lindhard[1–4] to later non-perturbative methods on model systems[5–8]. However, it is only recently that numerical methods[9] can directly tackle effects in the electronic stopping arising from the details of a realistic electronic structure of the host material at low projectile velocities, $v \ll v_\mathrm{Fermi}$. With the advent of these new methods, Pruneda *et al.*[10] investigated threshold effects in wide-band gap insulators, Zeb *et al.*[11] studied the electronic stopping power in Gold (the role of d electrons and the H/He anomaly), Lim *et al.*[12] discovered the role of dynamical interstitial levels in semiconductors and Quashie *et al.*[13] unveiled the effects of d-band electrons in copper. In these later cases, band structure effects, difficult to incorporate in early electronic stopping models are accounted for and shown to play a fundamental role[14].

Overall, the research mentioned above illustrates that the path towards low velocities of electronic stopping is not as simple (*e.g.* smooth and linear in v) as phenomenological models suggest[15]. The experimental evidence of deviations from linear velocity behavior and, for example, the role of d electrons was studied in Refs.[16–23]. Specifically for a copper host, a crossover region of superlinear velocity dependence (with a power of ~ 1.5) in the velocity range $v = 0.07 - 0.3$ a.u. ($0.12 - 2.2$ keV) of the electronic stopping of protons was shown to be associated to the copper electronic band structure, and in particular to the sharply peaked d-band located at ~ 2 eV below the Fermi energy[13].

In terms of electronic band structure effects, a nickel host presents a more singular situation than copper, because the Fermi level is precisely at the edge of the d-band (see Fig. 5 in Ref.[24]). This gives rise to the intriguing possibility that the electronic stopping is superlinear even at extremely low velocities[25].

Additionally, nickel has shown important technological applications stemming from its resistance to particle radiation, as it was recently discovered that Ni-based random alloys can withstand swelling under particle radiation. Ni based alloys are known for their radiation tolerance, thermal stability and optimal mechanical properties, making them promising candidate materials for nuclear applications[26].

In this paper, the case of S_e with emphasis on the low velocity limit of a nickel host under proton and alpha irradiation is presented. The comparison between proton and alpha irradiation helps understand the non-linear effects in the dielectric response and scaling laws with respect the projectile charge Z_1.

The stopping power of protons and He_4^+ ions in nickel in the energy range of 20 to 95 keV was studied experimentally in detail by Bogdanov *et al.*[27]. Their measured results for energy losses of protons in nickel are in good agreement with those of Refs.[28,29] but in less agreement with Ref.[30]. These disagreements among experiments may stem from scaling issues related to measuring relative and absolute S_e. The measured energy losses of He_4^+ ions in nickel[27] are in good agreement with the measurements of Ref.[31].

Møller *et al.*[32] measured the stopping power of antiprotons (and protons) in various solid targets in the low-energy range of $1 - 100$ keV. They found the stopping power of protons to be proportional to the projectile velocity below the stopping-power maximum for the Ni target and simply compare the observation with a free electron gas model.

In this work we employed the first principles time-dependent Kohn-Sham formalism of time-dependent density functional theory (TDDFT)[35] coupled with nuclei motion[36,37] to simulate the collision dynamics of two different projectiles (hydrogen/proton and helium/alpha particles) in Ni target. The electron dynamics is treated quantum mechanically whereas the nuclei are point particles treated classically.

The exchange-correlation potential used in this study is due to the local-density approximation (LDA) of density functional theory (DFT)[38]. More sophisticated approaches based on the dielectric response, including the exact many-body and dynamic exchange-correlation treatment for low velocity projectiles, are available in the literature[39,40] and shown to be important for the stopping at least in the specific case of the *homogeneous* electron gas.

This *atomistic* calculation used a supercell with volume $(19.98\ a_0)^3$, containing 108 fcc host Ni atoms (experimental density) plus the projectile. Periodic boundary conditions along with Ewald-type summation[43–46] are used throughout this study. The plane-wave basis set is sampled accurately with a 160 Ry energy cutoff. For some selected velocities we tested k-point convergence in a $(3 \times 3 \times 3)$- and a $(4 \times 4 \times 4)$-Monkhorst-Pack grid[47], with a negligible difference of less than 0.1%. Finite size effects were studied for 108 and 256 atoms in a supercell of $(3 \times 3 \times 3)$ and $(4 \times 4 \times 4)$ respectively, and the errors remain within 3%[13,48].

We used norm-conserving Troullier-Martins pseudopotential to represent ion potentials V_{ext}, with 10 and 16 (to assess semi-core effects) explicit electrons per Ni atom. The calculations were done using the QBOX code[41] with custom time-dependent modifications[9,42].

Initially, the projectiles (H or He) were placed in the Ni crystal interstitially to obtain a converged ground state by performing a *time-independent* DFT calculation. For the subsequent evolution of the moving projectile, a TDDFT calculation was then performed on the electronic system and the moving projectile. The projectile trajectory in the bulk crystal was done in two different ways: (i) hyper-channeling trajectory and (ii) off-channeling trajectory. In (i), the projectile is allowed to move with a given velocity subjected to a straight uniform movement along a ⟨100⟩ channel. This setup avoids collisions with target atoms[10,13,48–50]. In (ii), the projectile is forced to move in a *random* direction through the host material[13]. In this case, there is a stronger interaction between projectile and tightly bound electronic charge density in the vicinity of the host nuclei[13,48].

The wavefunctions are propagated in time using the fourth-order Runge-Kutta scheme[9] and the enforced time-reversal symmetry (ETRS)[51] method. The latter is more efficient for low projectile velocity calculations. We used these time integrators to ensure accurate propagation and forces at very low velocities. The propagation time step was set to, at most, 0.0242 attoseconds to ensure stable numerical integration[9,52].

As the projectile position changes with time, energy is being deposited into the electronic subsystem. This increase in total electronic energy E as a function of projectile displacement is identified as the S_{e} given by the trajectory average[53]:

$$S_{\mathrm{e}} = \left\langle \frac{\mathrm{d}E[x(t)]}{\mathrm{d}x(t)} \right\rangle \tag{1}$$

The calculated S_{e} for H^+ and He in Ni for a wide range of projectile velocities compared with empirical models and data are presented in Fig. 1. In the channeling case, where the projectile is forced to move in a straight path avoiding head on collisions with the host atoms; the calculated S_{e} is systematically lower than that of experiments for both projectiles. We attribute this difference to the fact that the projectile lacks access to the full variety of trajectories that an experiment with uncontrolled directionality (e.g. with respect to a well defined crystal orientation) would provide.

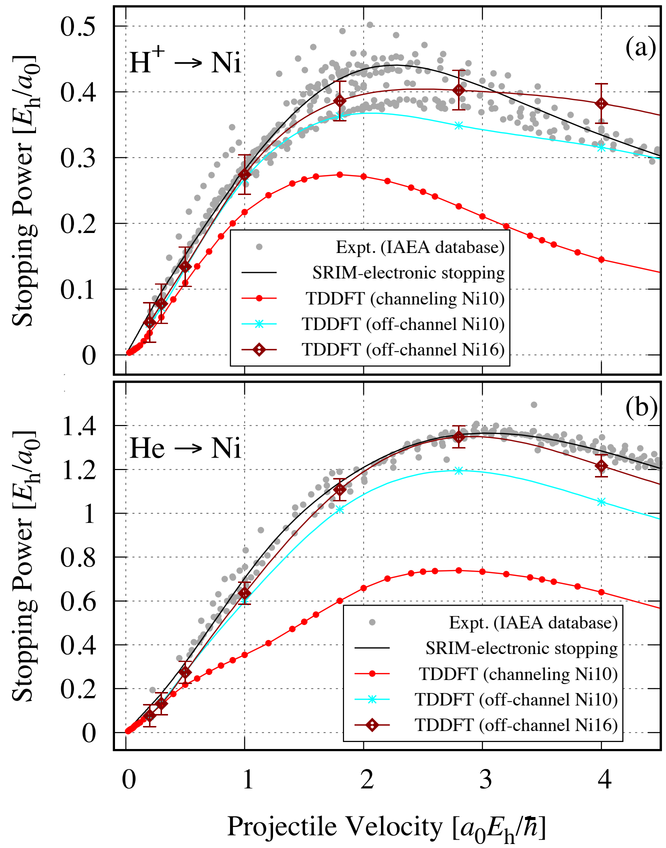

Figure 1. (color online). H^+ and He → Ni. The average S_{e} for (a) H^+ and (b) He versus projectile velocity v: for channeling trajectory (red filled circles) without semi-core, $[\mathrm{Ar}]3d^8 4s^2$ (10 valence electrons) denoted as 'TDDFT (channeling Ni10)', off-channeling trajectory (cyan asterisk) without semi-core, $[\mathrm{Ar}]3d^8 4s^2$ (10 valence electrons) denoted as 'TDDFT (off-channel Ni10)' and off-channeling trajectory with semi-core, $[\mathrm{Ne}\ 3s^2]3p^6 3d^8 4s^2$ (16 valence electrons) denoted as 'TDDFT (off-channel Ni16)'. The black continuous line refers to the empirically-based tabulated electronic-stopping power model from SRIM[15,54]. The gray dots refer to the IAEA experimental database[55].

We also performed simulations in off-channeling conditions where we allow the projectile to move in random directions, possibly closer to the host atoms. In most experimental setups, the projectiles are not channeled in any specific direction but rather are allowed to move in different directions and therefore explore different parts of the lattice. The use of random directions here are to specifically mimic the experimental setup, and was shown to work for other systems[13,48]. Doing so allows the projectile to seldom access core regions around the host atoms and thereby causing excitation of tightly bound electrons. Off-channeling trajectories are statistical in nature; averaging over different directions produce average values for stopping with a certain variance (shown as error bars in the graphs). The effective way to explore off-channeling trajectories is moving the projectile at several impact parameters (initial positions) and several velocity directions; and averaging over these different projectile initial positions and velocity directions. Here we used two main velocity incommensurate directions [0.309, 0.5, 0.809] and [0.705, 0.610, 0.363], with their corresponding permutations making a total of 12 velocity directions to obtain our off-channeling results.

In the off-channeling trajectories case, we studied two levels of pseudopotentials. First, we simulated the electronic system with a pseudopotential not including semi-core electrons in the valence (10 electrons per host atoms, $3d^8 4s^2$), while the rest of electrons, in particular the $3p^6$, are frozen and taken into account only as part of the pseudopotential. Second, to assess the role of semicore electrons we used a different pseudopotential including some semi-core electrons in valence; we simulated 16 electrons ($3p^6 3d^8 4s^2$) per host atom. In the calculation, the charge of the projectile is not chosen a *priori*; in the steady state the average charge state of the projectile is determined by the time-evolution of the system.

For H^+ in Fig. 1a, we obtained fairly good agreement with experiment in a wide range of velocities, as long as we consider off-channeling and include host semicore electrons explicitly. Semicore electron effects kick in at $v > 1.5$ a.u. and the correction is similar ($\sim 10\%$) in both cases (H^+ and He). The difference between off-channeling and channeling is appreciable for $v > 1.0$ a.u., and is particularly important in the case of alpha projectiles; although, it is seen that at velocities above 3.0 a.u. our off-channeling results go over the experimental data. On the other hand, the agreement obtained with experiment is excellent for $v \leq 3.0$ a.u. for He in Fig. 1b. At $v > 3.0$ a.u., our results underestimates experiment, indicating even more semicore electrons needs to be incorporated in the Ni pseudopotential if we were to explore higher velocities[56]. At lower velocities, both channeling and off-channeling trajectories collapse into one curve; this apparent independence on the geometry of the trajectory follows a pattern observed in previous simulations[13,50,57].

In Fig. 2 and 3 we concentrate in the low velocity limit and compare with the available experimental data and theory. In Fig. 2, for the range $0.2 < v < 5$ a.u. our calculated S_e for off-channeling proton is compared with experiments[15,27,32,58,59]. As an example, for $v \sim 0.2$ a.u. our channeling result is $\sim 10\%$ below compared with Andersen *et al.*[59]. There is little experimental data for $v < 0.2$ a.u.. However, $v \sim 0.08$ a.u., our TDDFT(channeling Ni10) result for protons is in good agreement with Arkhipov *et al.*[60] with 5% difference.

In Fig. 3, our results showed that the relatively

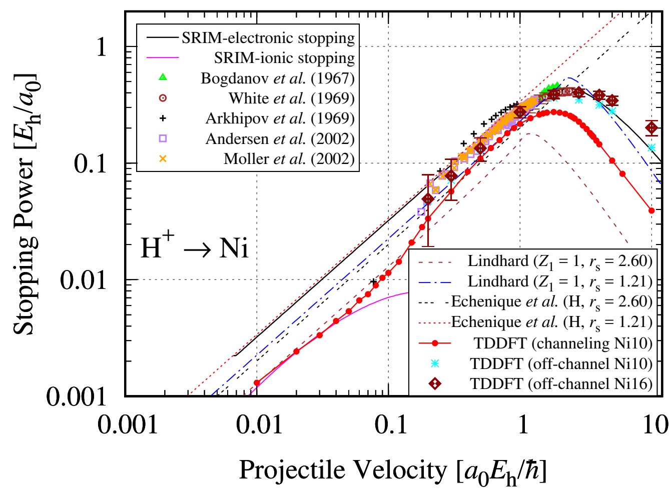

Figure 2. (color online). $H^+ \to$ Ni (log scale). The average S_e versus projectile velocity v for a channeling trajectory (red circles) without semi-core, [Ar]$3d^8 4s^2$ (10 valence electrons) denoted as 'TDDFT (channeling Ni10)', off-channeling trajectory (cyan asterisk) without semi-core, [Ar]$3d^8 4s^2$ (10 valence electrons) denoted as 'TDDFT (off-channel Ni10)', and off-channeling trajectory with semi-core, [Ne $3s^2$]$3p^6 3d^8 4s^2$ (16 valence electrons) denoted as 'TDDFT (off-channel Ni16)'. Dash (brown) line and dash-dot (blue) line corresponds to a linear RPA-based calculation for a free-electron gas with $r_\mathrm{s} = 2.60\ a_0$ and $r_\mathrm{s} = 1.21\ a_0$ where the effective charge of H^+ projectile is $Z_1 = 1$ (Eq. 2). Dash-dash (black) line and dot (red) line corresponds to DFT results (slopes) for proton by Echenique *et al.*[7] (see Fig. 3, curve 'D') with $r_\mathrm{s} = 2.60\ a_0$ and $r_\mathrm{s} = 1.21\ a_0$ (which nominally corresponds to 1 and 10 electrons per Ni atom respectively). The tabulated results from SRIM empirical model for the electronic and ionic stopping powers of protons are represented by the solid black and solid magenta lines, respectively[15].

heavier He projectile agrees well with Sillanpää *et al.*[33] (an indirect experimental result) in their velocity range (0.01 a.u. $\leq v \leq$ 0.1 a.u.). More experimental work in this velocity regime would be required to validate the capability of our ab initio TDDFT method. The lack of experimental data at $v < 0.01$ a.u. makes it difficult to validate our predictive result below this velocity regime. For higher velocity, our calculated results are in agreement with experimental data[27,33,58,61–63].

To analyze the behavior of the simulated S_e in detail, we evaluated the linear response stopping based on the Lindhard dielectric function for a homogeneous electron gas for effective electronic densities n[4,64–67]:

$$S_\mathrm{L}(n, v) = \frac{2Z_1^2 e^2}{\pi v^2} \int_0^\infty \frac{\mathrm{d}k}{k} \int_0^{kv} \omega \mathrm{d}\omega \Im \left(\varepsilon_\mathrm{RPA}[n, k, \omega]^{-1} \right), \tag{2}$$

where Z_1 is the charge of the projectile (ion) (for example, $Z_1 = 1$ for H^+ and $Z_1 = 2$ for a *fully stripped* He^{2+} ion), v is the velocity of the projectile and ε_RPA is a model of the dielectric function for the linear re-

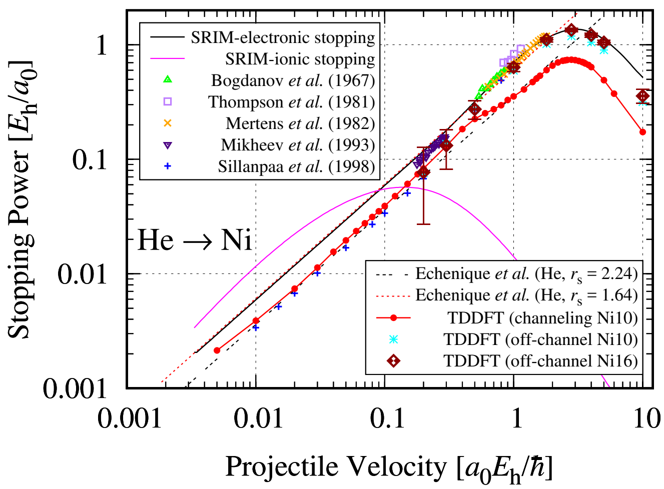

Figure 3. (color online). He → Ni (log scale). The average S_e versus projectile velocity v: for a channeling trajectory (red circles) without semi-core, $[Ar]3d^8 4s^2$ (10 valence electrons) denoted as 'TDDFT (channeling Ni10)' and for off-channeling trajectory (cyan asterisk) without semi-core, $[Ar]3d^8 4s^2$ (10 valence electrons) denoted as 'TDDFT (off-channel Ni10)', and off-channeling trajectory with semi-core, $[Ne\ 3s^2]3p^6 3d^8 4s^2$ (16 valence electrons) denoted as 'TDDFT (off-channel Ni16)'. Dash-dash (black) line and dot (red) line corresponds to DFT results (slopes) for a helium nucleus by Echenique *et al.*[7] with adjusted $r_s = 2.24\ a_0$ and $r_s = 1.64\ a_0$ (which nominally corresponds to 1.57 and 4 electrons per Ni atom respectively). The tabulated results from SRIM database for the electronic and ionic stopping powers of are represented by the solid black and solid magenta lines, respectively[15].

sponse approximation (RPA) at frequency ω and momentum transfer k for an electron gas with effective density n[68]. The linear-response approximation to the stopping power is relatively crude compared to the TDDFT simulation results presented here, but we compare the two here to understand with a simpler model our full TDDFT calculations in different limits. In order to compare to a more elaborate model we compare it with non-linear DFT calculations of stopping power which are formally exact for the homogeneous electron gas in the limit of $v \to 0$ reported in[7] for both H and He and parametrized by density n. For reference, we used $n = 9.1\times10^{22}/\text{cm}^3$, $n = 36.6\times10^{22}/\text{cm}^3$, $n = 91.4\times10^{22}/\text{cm}^3$ and $n = 146.2\times10^{22}/\text{cm}^3$ corresponding nominally to $1e$ ($r_s = 2.60\ a_0$), $4e$ ($r_s = 1.64\ a_0$), $10e$ ($r_s = 1.21\ a_0$) and $16e$ ($r_s = 1.03\ a_0$) electrons per Ni atom respectively.

In Fig. 2 our simulated TDDFT results at low velocities for proton projectiles corresponds well with linear response stopping (S_L) where $r_s = 2.60\ a_0$ ($Z_1 = 1$). Our TDDFT results agrees well with DFT results of Echenique *et al.* (see Fig. 3, curve 'D' of Ref.[7]) for $r_s = 1.21\ a_0$ around 0.2 a.u. $\leq v \leq$ 1.0 a.u. but at lower velocities ($v <$ 0.1 a.u.) their DFT results for $r_s = 2.60\ a_0$ overestimates our TDDFT results. Although there are two independent parameters to adjust in the Lindhard model (Z_1 and n), a picture in which $Z_1 \equiv 1$ (independent of velocity) seems reasonable for protons, since hydrogen loses its electron easily in a metallic environment[69].

We observe that for protons, S_e falls to values near the nuclear stopping estimated by the most current version of SRIM. Also according to our results, SRIM extrapolation ($v \to 0$) model is systematically overestimating the electronic stopping by a factor 2 or 3 for both types of projectiles. We again observe a crossover region (as seen in Cu result[13]). For 0.15 a.u. $\leq v \leq$ 0.5 a.u. crossover region, the curve is a power-law $\propto v^q$ where $q = 1.32$. We do not find non-linearities as a function of velocity below 0.15 a.u. in agreement with the expected analytic result for normal metallic stopping power.

For He, the linear response approximation is out of range at low velocity because of the dominance of non-linear effects and variable effective charges. For this reason, in Fig. 3 we only rely on the non-linear DFT ($v \to 0$) slopes reported by Echenique *et al.*, (see Fig. 3, curve 'E' in Ref.[7]) which agrees well with our TDDFT result when an adjusted $r_s = 2.24\ a_0$ is used, which in turn corresponds to $Z_1^* = 1.2$ (according to Fig. 4 in Ref.[7]). At higher velocity the comparison is not as straight forward but a preliminary adjustment to Ref.[7] gives an effective $r_s = 1.64\ a_0$ and $Z_1^* = 1.5$ respectively, for 0.5 a.u. $< v <$ 2.0 a.u. (off-channeling). That is, more charge is being stripped off from the He projectile and more valence electrons participate[70].

In summary, we obtained accurate results for the electronic stopping power of protons and alpha particles in Nickel. Despite the d-band being very close to the Fermi energy, the electronic stopping does not follow an anomalous electronic stopping power in the limit $v \to 0$. The electronic stopping power is linear with the velocity, similar to the linear response of the homogeneous electron gas. As in the case of Cu[13] we observe a crossover region of superlinear stopping power for the proton in Ni, but only for $v >$ 0.15 a.u..

In the case of the alpha particle, the stopping power is more linear with respect to velocity. There is no crossover region for alpha, and the only feature appears at $v >$ 0.5 a.u., due to the consideration of off-chanelling trajectories.

The resulting stopping power is in surprisingly good agreement with the experimental determinations at extremely low velocities for both protons and alpha particles [33,60], even when utilizing the simple adiabatic local density approximation (ALDA) to the electronic exchange correlation. Although non-local theories based on many-body physics for dynamic exchange-correlation, were previously shown to be necessary in the case of the homogeneous electron gas in the limit of low velocity[39,40], we achieved the *ab initio* calculation of electronic stopping power at the lowest velocity to date and we do not seem to find further corrections to exchange-correction to be a key element to account for in the calculation of electronic stopping in for these projectiles and realistic materials.

We thank J.M. Pitarke for constructive discussions of the nonlocal exchange-correlation in time-dependent current density functional theory. This work was performed under the auspices of the U.S. Department of Energy by Lawrence Livermore National Laboratory under Contract DE-AC52-07NA27344 and funded by the Energy Dissipation to Defect Evolution Center, EDDE, an Energy Frontier Research Center of the U.S. Department of Energy. Computing support for this work came from the Lawrence Livermore National Laboratory Institutional Computing Grand Challenge program.

---

[1] H. Bethe, Annalen der Physik **397**, 325 (1930).
[2] F. Bloch, Annalen der Physik **408**, 285 (1933).
[3] E. Fermi and E. Teller, Physical Review **72**, 399 (1947).
[4] J. Lindhard, Physics Letters **12**, 126 (1964).
[5] P. Echenique, R. Nieminen, and R. Ritchie, Solid State Communications **37**, 779 (1981).
[6] M. J. Puska and R. M. Nieminen, Physical Review B **27**, 6121 (1983).
[7] P. M. Echenique, R. M. Nieminen, J. C. Ashley, and R. H. Ritchie, Physical Review A **33**, 897 (1986).
[8] P. M. Echenique, I. Nagy, and A. Arnau, International Journal of Quantum Chemistry **36**, 521 (2009).
[9] A. Schleife, E. W. Draeger, Y. Kanai, and A. A. Correa, The Journal of Chemical Physics **137**, 22A546 (2012).
[10] J. M. Pruneda, D. Sánchez-Portal, A. Arnau, J. I. Juaristi, and E. Artacho, Physical Review Letters **99** (2007), 10.1103/physrevlett.99.235501.
[11] M. A. Zeb, J. Kohanoff, D. Sánchez-Portal, A. Arnau, J. I. Juaristi, and E. Artacho, Physical Review Letters **108** (2012), 10.1103/physrevlett.108.225504.
[12] A. Lim, W. Foulkes, A. Horsfield, D. Mason, A. Schleife, E. Draeger, and A. Correa, Physical Review Letters **116** (2016), 10.1103/physrevlett.116.043201.
[13] E. E. Quashie, B. C. Saha, and A. A. Correa, Physical Review B **94** (2016), 10.1103/physrevb.94.155403.
[14] E. Artacho, Journal of Physics: Condensed Matter **19**, 275211 (2007).
[15] J. F. Ziegler, M. Ziegler, and J. Biersack, Nuclear Instruments and Methods in Physics Research Section B: Beam Interactions with Materials and Atoms **268**, 1818 (2010).
[16] R. BLUME, W. ECKSTEIN, and H. VERBEEK, in *Ion Beam Analysis* (Elsevier, 1980) pp. 57–62.
[17] J. E. Valdés, J. C. Eckardt, G. H. Lantschner, and N. R. Arista, Physical Review A **49**, 1083 (1994).
[18] E. A. Figueroa, E. D. Cantero, J. C. Eckardt, G. H. Lantschner, J. E. Valdés, and N. R. Arista, Physical Review A **75** (2007), 10.1103/physreva.75.010901.
[19] S. N. Markin, D. Primetzhofer, S. Prusa, M. Brunmayr, G. Kowarik, F. Aumayr, and P. Bauer, Physical Review B **78** (2008), 10.1103/physrevb.78.195122.
[20] E. D. Cantero, R. C. Fadanelli, C. C. Montanari, M. Behar, J. C. Eckardt, G. H. Lantschner, J. E. Miraglia, and N. R. Arista, Physical Review A **79** (2009), 10.1103/physreva.79.042904.
[21] D. Goebl, D. Roth, and P. Bauer, Physical Review A **87** (2013), 10.1103/physreva.87.062903.
[22] D. Roth, B. Bruckner, M. Moro, S. Gruber, D. Goebl, J. Juaristi, M. Alducin, R. Steinberger, J. Duchoslav, D. Primetzhofer, and P. Bauer, Physical Review Letters **118** (2017), 10.1103/physrevlett.118.103401.
[23] D. Roth, B. Bruckner, G. Undeutsch, V. Paneta, A. Mardare, C. McGahan, M. Dosmailov, J. Juaristi, M. Alducin, J. Pedarnig, R. Haglund, D. Primetzhofer, and P. Bauer, Physical Review Letters **119** (2017), 10.1103/physrevlett.119.163401.
[24] Z. Lin, L. V. Zhigilei, and V. Celli, Physical Review B **77** (2008), 10.1103/physrevb.77.075133.
[25] J. M. Fernández-Varea and N. R. Arista, Radiation Physics and Chemistry **96**, 88 (2014).
[26] Y. Zhang, K. Jin, H. Xue, C. Lu, R. J. Olsen, L. K. Beland, M. W. Ullah, S. Zhao, H. Bei, D. S. Aidhy, G. D. Samolyuk, L. Wang, M. Caro, A. Caro, G. M. Stocks, B. C. Larson, I. M. Robertson, A. A. Correa, and W. J. Weber, Journal of Materials Research **31**, 2363 (2016).
[27] G. F. Bogdanov, V. P. Kabaev, F. V. Lebedev, and G. M. Novikov, Soviet Atomic Energy **22**, 133 (1967).
[28] A. B. Chilton, J. N. Cooper, and J. C. Harris, Physical Review **93**, 413 (1954).
[29] M. Bader, R. E. Pixley, F. S. Mozer, and W. Whaling, Physical Review **103**, 32 (1956).
[30] G. M. Osetinskii, Supplement No. 5 to Atomnaya Énergiya. [in Russian] Moscow, Atomizdat **94**, 5 (1957).
[31] S. K. Allison, Reviews of Modern Physics **30**, 1137 (1958).
[32] S. P. Møller, A. Csete, T. Ichioka, H. Knudsen, U. I. Uggerhøj, and H. H. Andersen, Physical Review Letters **88** (2002), 10.1103/physrevlett.88.193201.
[33] J. Sillanpää, E. Vainonen-Ahlgren, P. Haussalo, and J. Keinonen, Nuclear Instruments and Methods in Physics Research Section B: Beam Interactions with Materials and Atoms **142**, 1 (1998).
[34] J. F. Ziegler, U. Littmark, and J. P. Biersack. *The stopping and range of ions in solids*, volume 1. Pergamon New York, 1985. URL `https://nla.gov.au/nla.cat-vn125402`.
[35] C. A. Ullrich, *Time-Dependent Density-Functional Theory* (Oxford University Press, 2011).
[36] E. K. U. Gross, J. F. Dobson, and M. Petersilka, in *Topics in Current Chemistry* (Springer-Verlag) pp. 81–172.
[37] X. Andrade, A. Castro, D. Zueco, J. L. Alonso, P. Echenique, F. Falceto, and Á. Rubio, Journal of Chemical Theory and Computation **5**, 728 (2009).
[38] J. P. Perdew and A. Zunger, Physical Review B **23**, 5048 (1981).
[39] V. U. Nazarov, J. M. Pitarke, C. S. Kim, and Y. Takada, Physical Review B **71** (2005), 10.1103/physrevb.71.121106.
[40] V. U. Nazarov, J. M. Pitarke, Y. Takada, G. Vignale, and Y.-C. Chang, Physical Review B **76** (2007), 10.1103/physrevb.76.205103.
[41] F. Gygi, IBM Journal of Research and Development **52**, 137 (2008).
[42] E. W. Draeger, X. Andrade, J. A. Gunnels, A. Bhatele, A. Schleife, and A. A. Correa, in *2016 IEEE International Parallel and Distributed Processing Symposium (IPDPS)* (IEEE, 2016).

[43] J. Kolafa and J. W. Perram, Molecular Simulation **9**, 351 (1992).
[44] H. D. Herce, A. E. Garcia, and T. Darden, The Journal of Chemical Physics **126**, 124106 (2007).
[45] B. A. Wells and A. L. Chaffee, Journal of Chemical Theory and Computation **11**, 3684 (2015).
[46] A. Bródka, Chemical Physics Letters **400**, 62 (2004).
[47] Hendrik J. Monkhorst and James D. Pack. Special points for Brillouin-zone integrations. *Physical Review B*, 13(12): 5188–5192, jun 1976. doi:10.1103/physrevb.13.5188. URL https://doi.org/10.1103%2Fphysrevb.13.5188.
[48] A. Schleife, Y. Kanai, and A. A. Correa, Physical Review B **91** (2015), 10.1103/physrevb.91.014306.
[49] J. M. Pruneda and E. Artacho, Physical Review B **71** (2005), 10.1103/physrevb.71.094113.
[50] A. A. Correa, J. Kohanoff, E. Artacho, D. Sánchez-Portal, and A. Caro, Physical Review Letters **108** (2012), 10.1103/physrevlett.108.213201.
[51] A. Castro, M. A. L. Marques, and A. Rubio, The Journal of Chemical Physics **121**, 3425 (2004).
[52] Adrián Gómez Pueyo, Miguel A. L. Marques, Angel Rubio, and Alberto Castro. Propagators for the Time-Dependent Kohn–Sham Equations: Multistep Runge–Kutta, Exponential Runge–Kutta, and Commutator Free Magnus Methods. *Journal of Chemical Theory and Computation*, 14(6):3040–3052, apr 2018. doi:10.1021/acs.jctc.8b00197. URL https://doi.org/10.1021%2Facs.jctc.8b00197.
[53] Alfredo A. Correa. Calculating electronic stopping power in materials from first principles. *Computational Materials Science*, 150:291–303, jul 2018. doi: 10.1016/j.commatsci.2018.03.064. URL https://doi.org/10.1016%2Fj.commatsci.2018.03.064.
[54] J. F. Ziegler, http://www.srim.org/SRIM/SRIMPICS/STOP01/STOP0128.gif.
[55] Stopping Power of Matter for Ions Graphs, Data, Comments and Programs, (last updated Dec 18, 2017) http://www-nds.iaea.org/stopping/stopping_hydr.html.
[56] Rafi Ullah, Emilio Artacho, and Alfredo A. Correa. Core Electrons in the Electronic Stopping of Heavy Ions. *Physical Review Letters*, 121(11), sep 2018. doi: 10.1103/physrevlett.121.116401. URL https://doi.org/10.1103%2Fphysrevlett.121.116401.
[57] R. Ullah, F. Corsetti, D. Sánchez-Portal, and E. Artacho, Physical Review B **91** (2015), 10.1103/physrevb.91.125203.
[58] W. White and R. M. Mueller, Physical Review **187**, 499 (1969).
[59] H. Andersen, A. Csete, T. Ichioka, H. Knudsen, S. Møller, and U. Uggerhøj, Nuclear Instruments and Methods in Physics Research Section B: Beam Interactions with Materials and Atoms **194**, 217 (2002).
[60] E. P. Arkhipov and Y. V. Gott, Sov. Phys. JETP **29**, 615 (1969).
[61] S. Mikheev, Y. Ryzhov, I. Shkarban, and V. Yurasova, Nuclear Instruments and Methods in Physics Research Section B: Beam Interactions with Materials and Atoms **78**, 86 (1993).
[62] D. Thompson, W. Poehlman, P. Presunka, and J. Davies, Nuclear Instruments and Methods in Physics Research **191**, 469 (1981).
[63] P. Mertens and T. Krist, Journal of Applied Physics **53**, 7343 (1982).
[64] J. Lindhard and M. Scharff, Kgl. Danske Videnskab. Selskab. Mat. Fys. Medd. **27**, 15 (1953).
[65] J. Lindhard and A. Winther, Kgl. Danske Videnskab. Selskab. Mat. Fys. Medd. **34**, 1 (1964).
[66] J. Lindhard, Kgl. Danske Videnskab. Selskab. Mat. Fys. Medd. **28**, 1 (1954).
[67] J. Lindhard and A. Winther, *Stopping Power of Electron Gas and Equipartition Rule*, Kongelige Danske vidensk-abernes selskab Mathematisk-fysiske meddelelser (Munksgaard, Copenhagen, 1964).
[68] G. Giuliani and G. Vignale. *Quantum Theory of the Electron Liquid*. Cambridge University Press, 2008. ISBN 9781139471589. URL https://books.google.com/books?id=FFydOyv_r78C.
[69] N. Arista, Mat. Fys. Medd. Kong. Dan. Vid. Selsk. **52**, 595 (2006).
[70] A. Arnau, M. Peñalba, P. Echenique, and F. Flores, Nuclear Instruments and Methods in Physics Research Section B: Beam Interactions with Materials and Atoms **69**, 102 (1992).